Astronomy & Astrophysics manuscript no. 080109n
September 4, 2009

Simultaneous polarization monitoring of the X-ray flash XRF 080109/SN 2008D and SN 2007uy: isolating geometry from dust

J. Gorosabel[1], A. de Ugarte Postigo[2,3], A.J. Castro-Tirado[1], I. Agudo[1], M. Jelínek[1], S. Leon[4], T. Augusteijn[5], J.P.U. Fynbo[6], J. Hjorth[6], M.J. Michałowski[6], D. Xu[6], P. Ferrero[7], D.A. Kann[7], S. Klose[7], A. Rossi[7], J.P. Madrid[8], A. LLorente[9], M. Bremer[10], and J.-M. Winters[10]

[1] Instituto de Astrofísica de Andalucía (CSIC), 18008 Granada, Spain.
[2] European Southern Observatory, Casilla 19001, Santiago 19, Chile.
[3] INAF/Osservatorio Astronomico di Brera, via Bianchi 46, 23807 Merate, LC, Italy.
[4] Instituto de Radioastronomía Milimétrica (IRAM), Avenida Divina Pastora 7, Núcleo Central, 18012 Granada, Spain.
[5] Nordic Optical Telescope, Apartado 474, 38700 Santa Cruz de La Palma, Spain.
[6] Dark Cosmology Centre, Niels Bohr Institute, University of Copenhagen, Juliane Maries Vej 30, 2100 Copenhagen Ø, Denmark.
[7] Thüringer Landessternwarte Tautenburg, Sternwarte 5, D-07778 Tautenburg, Germany.
[8] Department of Physics and Astronomy, McMaster University, Hamilton L8S 4M1, Canada.
[9] Herschel Science Operations Centre, European Space Agency, Villafranca del Castillo, PO Box 50727, 28080 Madrid, Spain.
[10] Institute de Radioastronomie Millimétrique (IRAM), 300 rue de la Piscine, 38406 Saint Martin d´Héres, France.

Received August 24, 2009

ABSTRACT

Context. There is a general consensus that Long Gamma-Ray Bursts (GRBs), including X-ray Flashes (XRFs), are created by the explosion of massive stars. However little is still known about the geometry of such stellar explosions. In this paper we study the optical polarimetric properties of an XRF dominated by the associated hypernova, in other words, an XRF with no contaminating afterglow. The final scope of this study is to shed light on the still uncertain picture of the GRBs' expansion geometry.
Aims. The main aim is to investigate the evolution of the linear optical polarization of the X-ray flash XRF 080109/SN 2008D. As a secondary product, we also report the polarization evolution of SN 2007uy, and discuss the properties of the host galaxy interstellar medium (ISM) towards the XRF.
Methods. We present a *V*-band linear polarization monitoring campaign carried out for the X-ray flash XRF 080109/SN 2008D and SN 2007uy, which shone for weeks contemporaneously in NGC 2770. This fortunate coincidence brought us the opportunity to observe both objects simultaneously, and most importantly, with identical instrumental setups. The observations span 74.9 days, starting 3.6 days after the X-ray flash and are distributed in 11 visits. In addition we performed observations in the millimetre (mm) range in order to identify the dominant origin of the observed polarization.
Results. We report positive linear polarization detections at several epochs for XRF 080109/SN 2008 at a level of ∼1%. For SN 2007uy the measured polarization is around ∼ 1.5%. In both cases the observed linear polarization seems dominated by the host galaxy interstellar polarization (HGIP), especially for the case of SN 2007uy. Dust emission at 1.2 mm detected at and around the XRF position supports this scenario. Despite the dominant HGIP, a statistical analysis of the distribution of the XRF 080109/SN 2008D Stokes parametres suggests that it could show a possible intrinsic variable polarization component. Moreover we show that the temporal evolution of the intrinsic XRF 080109/SN 2008D polarization could be explained by an aspherical axisymmetric expansion with variable eccentricity, although other more complex geometric scenarios are also compatible. In contrast, the SN 2007uy polarization could be described by the HGIP plus a constant eccentricity expansion on the plane of the sky. We suggest that at least the projected, if not the intrinsic, geometry of XRF 080109/SN 2008D and SN 2007uy could be different.

Key words. Gamma rays: bursts – Techniques: polarimetry

1. Introduction

It is well established that long duration gamma-ray bursts (LGRBs) are produced by the explosive death of massive stars (Hjorth et al. 2003; Stanek et al. 2003). The LGRBs with the lowest peak-energies are classified as X-ray flashes (XRFs; Sakamoto et al. 2005).

LGRBs with optical emission dominated by the associated supernova (hereafter named as pure hypernova, or PHN[1]) are rarely detected (Galama et al. 1998; Malesani et al. 2004; Thomsen et al. 2004; Pian et al. 2006; Soderberg et al. 2008; see also for a review Woosley & Bloom 2006). This is in contrast to the hundreds of LGRBs discovered to date which are dominated by their afterglows (see for instance, Kann et al. 2007, Kann et al. 2008, Fynbo et al. 2009, or J. Greiner's GRB list[2]). In the same way, broad-band polarization observations have been carried out for a significant amount of afterglows (Covino et al. 1999; Hjorth et al. 1999; Covino et al. 2002; Bersier et al. 2003; Björnsson et al. 2003; Covino et al. 2003; Greiner et al. 2003; Masetti et al. 2003; Rol et al. 2003; Gorosabel et al. 2004, see also the recent review

[1] Hereafter we use the term PHN to refer to a stellar explosion with detected prompt high-energy emission (γ or/and X-rays) with a negligible contaminating afterglow. Hence, for instance GRB 030329 would not be a PHN, but instead GRB 031203, GRB 980425 and XRF 060218 would be considered as PHNe.

[2] Available at `http://www.mpe.mpg.de/~jcg/grbgen.html`

by Covino 2009), however broad-band polarization detections of PHNe have been very sparse (Gorosabel et al. 2006) and therefore potentially valuable.

Given the very few broad-band polarimetric studies carried out for PHNe to date, any new observation could contribute to gain an insight into the GRB phenomena. In these unique cases the lack of a contaminating afterglow allows to use PHNe to elucidate the expansion geometry of GRB progenitors. XRF 080109/SN 2008D is one of those rare events. Following the scheme proposed by Sollerman et al. (2006), XRF 080109/SN 2008D can be classified as a PHN with the high-energy properties of an X-ray flash. Thus, the study through polarimetric data of the expansion geometry of events like XRF 080109/SN 2008D could shed light on the still uncertain geometrical configuration in the first stages of the GRB collapse (Woosley 1993; MacFadyen & Woosley 1999).

XRF 080109 was serendipitously discovered on January 9.56446 UT by *Swift* as a bright X-ray outburst during a scheduled observation of SN 2007uy (Berger & Soderberg 2008; Kong & Maccarone 2008; Immler et al. 2008; Soderberg et al. 2008). In the optical both XRF 080109/SN 2008D and SN 2007uy shone contemporaneously for weeks in the nearby ($z = 0.007$) spiral galaxy NGC 2770. This fortunate coincidence brought us the opportunity to observe both objects simultaneously, and most importantly, with the same instrumental setup. XRF 080109 was attributed to the shock breakout emission from SN 2008D, classified as a He-rich Ibc supernova (SN) (Soderberg et al. 2008; Malesani et al. 2009; Modjaz et al. 2009). XRF 080109/SN 2008D represents a transition between the most energetic hypernovae (linked to canonical LGRBs) and standard core-collapse SNe (Mazzali et al. 2008). It is noticeable that spectroscopic observations of XRF 080109/SN 2008D suggested an aspherical expansion geometry (Modjaz et al. 2009; Tanaka et al. 2009). In fact it has been proposed that XRF 080109/SN 2008D is a side-viewed, bipolar explosion with a viewing angle of $> 50^\circ$ from the polar direction (Tanaka et al. 2009).

Recently Maund et al. (2009) have reported a spectropolarimetric study of XRF 080109/SN 2008D based on data acquired on January 31.22 and February 15.18 UT, close to two of our eleven observing epochs. One of the main advantages of spectropolarimetry of PHNe with respect to broad-band polarimetry is its ability to infer geometric and dynamical information for the different chemical constituents of the explosion. Broad-band polarimetric observations construct a rougher picture of the stellar death, but require lower signal-to-noise ratios than spectropolarimetry. So broad-band polarimetric observations can be extended to objects at higher redshifts or/and they allow to enhance the polarimetric coverage and sampling of the lightcurve, especially at epochs distant from the maximum when the PHN is dimmer.

The dominant intrinsic polarization in PHNe, is thought to originate by the same mechanism as in standard SNe; Thompson photon scattering through an aspherical photospheric expansion (Höflich et al. 1991). If the PHN photosphere projection on the sky plane is an ellipse, in general a non-cancelled linear polarization is expected perpendicular or parallel to the major axis (Kasen et al. 2003). If the expansion ellipticity evolves with time, keeping the direction of both axes, then the Stokes parametres should also move on a straight line of the Stokes plane (Wang et al. 2001). Once the Milky Way Galactic interstellar polarization (GIP) has been corrected, this straight line is expected to be displaced from the origin of the Stokes plane due to the host galaxy interstellar polarization (HGIP). The contribution of additional polarization components (variable line polarization, irruption of the stellar core, variable HGIP, etc...) can distort this rough ellipsoidal stellar picture, resulting in a more complex geometrical configuration (see Maund et al. 2009, and references therein). Asphericities in explosive stellar deaths tend to be low, usually yielding optical polarization values below $\sim 1\%$ (Wang & Wheeler 2008). However, counterexamples exist, such as the Ic-Type SN 1997X (Wang et al. 2001) or the PHN XRF 060218/SN 2006aj (Gorosabel et al. 2006; Maund et al. 2007).

In this paper we report optical polarimetric observations of XRF 080109/SN 2008D and SN 2007uy aimed at obtaining geometrical information on the expansion of these events. In addition we show the results of millimetre (mm) observations which were used to infer information about the host galaxy extinction and consequently about the HGIP impact on the observed polarization.

2. Observations and data analysis

2.1. Optical observations

Table 1 displays the log of our optical observations. All the data were taken in the *V*-band. The observations were carried out with the 2.2m Calar Alto telescope (CAHA), the 2.5m Nordic Optical Telescope (NOT) and the 8.2m Unit Telescope 2 of the Very Large Telescope (VLT).

The NOT observations were performed with ALFOSC, through a calcite and a 1/2 wave retarder plate. Four images of the field were acquired, rotating the retarder plate at 0°, 22.5°, 45.0° and 67.5°. The calcite plates reduce the ALFOSC field of view (FoV) to 140″ in diameter (pixel scale of 0.″19/pix). SN 2007uy was left out of the NOT images due to this reduced FoV.

The CAHA observations were based on the CAFOS instrument. The CAFOS polarization unit uses a Wollaston prism instead of a calcite plate and has a strip mask on the focal plane to avoid accidental overlapping on the CCD. The total FoV of CAFOS is composed by 14 strips of $9' \times 18''$ each, providing a large enough FoV to image both XRF 080109/SN 2008D and SN 2007uy simultaneously.

The VLT observations were done with FORS1, with a setup similar to CAFOS. As in CAFOS, the large FoV of FORS1 allowed us to image simultaneously XRF 080109/SN 2008D and SN 2007uy. In some of the FORS1 visits we used the 1×1 bin read-out mode in order to avoid saturation of SN 2007uy while keeping a high signal to noise ratio for XRF 080109/SN 2008D. We note that, in addition to the CCD binning, the seeing and transparency conditions varied significantly from night to night. This made it impossible to have a bright unsaturated field star common to all our images. Apart from XRF 080109/SN 2008D, SN 2007uy was the object most frequently imaged, being present in the FoV of all the FORS1 and CAFOS images. This fact provided us with the opportunity of using SN 2007uy as a polarimetric reference star on the Stokes plane (see discussion of Sect. 3.2).

The images were reduced using standard procedures running under IRAF[3]. The master flat field image was created combining sky flat field frames taken without polarization units in the

[3] IRAF is distributed by the National Optical Astronomy Observatory, which is operated by the Association of Universities for Research in Astronomy (AURA) under cooperative agreement with the National Science Foundation.

Table 1. Polarimetric observations of XRF 080109/SN 2008D and SN 2007uy.

Date[a]	Telescope	Exposure	Seeing	XRF 080109/SN 2008D			SN 2007uy[b]		
2008, UT	(+Instrument)	time (s)	($''$)	$P \pm \sigma_P$	$\theta \pm \sigma_\theta$	$V \pm \sigma_V^c$	$P \pm \sigma_P$	$\theta \pm \sigma_\theta$	$V \pm \sigma_V^c$
Jan 13.1644	NOT(+ALFOSC)	12×600	0.7	0.95 ± 0.20	114.9 ± 5.9	18.44 ± 0.05	———	———	———
				(0.95 ± 0.20)	(114.9 ± 5.9)		———	———	———
Jan 13.2642	VLT(+FORS1)	2330[d]	1.0	0.68 ± 0.22	119.2 ± 9.5	18.39 ± 0.05	1.45 ± 0.25	178.6 ± 4.6	15.78 ± 0.05
				(0.65 ± 0.33)[e]	(124.5 ± 13.3)		(1.59 ± 0.04)	(177.4 ± 0.7)	
Jan 15.0780	NOT(+ALFOSC)	12×600	0.9	0.85 ± 0.28	106.1 ± 9.4	18.28 ± 0.05	———	———	———
				(0.85 ± 0.28)	(106.1 ± 9.4)		———	———	———
Jan 17.2518	VLT(+FORS1)	8×285	1.0	0.84 ± 0.45	138.3 ± 8.1	17.90 ± 0.05	1.43 ± 0.14	182.5 ± 5.1	15.69 ± 0.05
				(1.14 ± 0.51)	(141.0 ± 7.2)		(1.59 ± 0.04)	(177.4 ± 0.7)	
Jan 30.1858	VLT(+FORS1)	4×285	0.8	1.05 ± 0.06	135.3 ± 1.7	17.31 ± 0.05	1.64 ± 0.06	178.5 ± 1.1	16.39 ± 0.05
				(1.11 ± 0.08)	(134.0 ± 2.0)		(1.59 ± 0.04)	(177.4 ± 0.7)	
Jan 30.2022	VLT(+FORS1)	4×285	0.8	1.28 ± 0.06	132.5 ± 1.4	17.27 ± 0.05	1.56 ± 0.06	176.1 ± 1.1	16.36 ± 0.05
				(1.21 ± 0.08)	(133.3 ± 1.9)		(1.59 ± 0.04)	(177.4 ± 0.7)	
Feb 11.9326	CAHA(+CAFOS)	13×400	2.0	1.58 ± 0.97	126.6 ± 16.4	17.82 ± 0.09	0.92 ± 0.88	179.8 ± 26.0	17.09 ± 0.11
				(1.19 ± 1.51)	(131.6 ± 20.5)		(1.59 ± 0.04)	(177.4 ± 0.7)	
Feb 26.1107	CAHA(+CAFOS)	16×600	1.9	$< 2.76^f$	———	18.52 ± 0.09	1.81 ± 0.63	173.5 ± 14.4	17.56 ± 0.08
				($< 2.94^f$)	———		(1.59 ± 0.04)	(177.4 ± 0.7)	
Feb 26.9444	NOT(+ALFOSC)	16×400	1.3	0.98 ± 0.80	124.6 ± 23.2	18.79 ± 0.08	———	———	———
				(0.98 ± 0.80)	(124.6 ± 23.2)		———	———	———
Mar 2.1102	VLT(+FORS1)	4×525	1.1	1.42 ± 0.46	139.0 ± 9.1	18.80 ± 0.05	1.83 ± 0.19	174.6 ± 3.2	17.55 ± 0.05
				(1.17 ± 0.51)	(134.7 ± 11.4)		(1.59 ± 0.04)	(177.4 ± 0.7)	
Mar 28.0207	VLT(+FORS1)	4×525	1.1	0.75 ± 0.57	111.2 ± 21.9	19.42 ± 0.05	1.58 ± 0.42	179.6 ± 7.6	17.98 ± 0.05
				(0.73 ± 0.78)	(112.7 ± 21.0)		(1.59 ± 0.04)	(177.4 ± 0.7)	

a Mean observing epoch.

b For the NOT visits SN 2007uy was out of the FoV, so the degree of linear polarization (P), the position angle (θ), and the magnitude (V) could not be determined.

c Calibration based on Malesani et al. (2009). The photometric errors include the zero point uncertainty.

d The polarimetric cycle was interrupted and restarted several times. The SN 2007uy observing epoch and the exposure time are slightly different from the XRF 080109/SN 2008D ones, corresponding to Jan 13.2708 UT and 990 seconds, respectively.

e The XRF 080109/SN 2008D P and θ values given for VLT and CAHA in between parentheses assume a constant SN 2007uy polarization given by $\langle P \rangle = 1.59 \pm 0.04$ and $\langle \theta \rangle = 177.4 \pm 0.7$.

f 1σ upper limit.

light path. This process was applied separately for the 3 instruments. In principle, the host galaxy background might pose a potential problem for the photometry accuracy of SN 2007uy and XRF 080109/SN 2008D. Thus we double checked the impact of the host galaxy background level determination by performing aperture photometry with radii ranging from 0.5 to 2.5 times the FWHM (Full Width at Half Maximum), and varying the inner radii of the background annuli from 3 to 5 times the FWHM. The annuli widths were also varied from 2.5 to 4 times the FWHM. We verified that the resulting Stokes parametres were consistent within error bars, independent of the apertures and annuli used. Then the apertures and annuli yielding minimum errors were adopted (typically the apertures and the inner radii used were the FWHM and 3-4 times the FWHM, respectively). In any case, in order to account for potential dismissed photometric error sources, the statistical analysis of Sect. 3.2.1 was duplicated considering also photometric errors augmented by 20%.

For the ALFOSC and CAFOS data the determination of the Stokes parametres was done by fitting the $S(\theta)$ function with the corresponding Milky Way GIP normalization factor (di Serego Alighieri 1997). The GIP normalization factor was calculated using Galactic field stars. In the case of FORS1 the Stokes parametres were calculated via Fourier expansion, in order to include the instrumental polarization dependence across the FoV (see FORS1 manual[4]).

Due to the reduced ALFOSC FoV only two unsaturated bright field stars were available for the GIP correction of the NOT data. Fortunately for the three NOT epochs the stars used for the NOT GIP correction remained the same. This assures internal consistency of the position of the NOT Stokes parametres on the Stokes plane. Thus, a potential relative shift (owing to different GIP corrections) of the NOT Stokes parametres with respect to each other was minimized. This fact will have its relevance in the further discussion since, as argued in Sect. 3.2.2, the polarimetric data might suggest the existence of a symmetry axis which is consistently determined by different instrumental setups.

The wider FoV of FORS1 and CAFOS provided a larger number of stars for the GIP correction than with ALFOSC. Due to different observing conditions (seeing, transparency and CCD binning) at VLT and CAHA the stars varied from one night to another. This was not critical for the FORS1 and CAFOS images, since the GIP correction for both XRF 080109/SN 2008D and SN 2007uy were always calculated using the same set of stars for each epoch. And most importantly, given that SN 2007uy was very well detected in all the VLT and CAHA images, we could use this object (justified by a statistical analysis, see Sect. 3.2.1) as a secondary calibrator and keep it fixed on the Stokes plane (see Sect. 3.2.2).

It is important to stress that the GIP corrections applied to the different data-sets were very similar since the Galactic extinction towards NGC 2770 is only $A_V = 0.1$ mag (Schlegel et al. 1998; Cardelli et al. 1989). So in all cases the GIP corrections applied were low ($\sim 0.2 - 0.3\%$), in agreement with the Galactic polarization predictions ($P_{max} = 2.9 \times A_V = 0.29\%$; Serkowski et al. 1975; Cardelli et al. 1989). In fact, the GIP cor-

[4] Doc. N. VLT-MAN-ESO-13100-1543 Issue 82.1, Date 27/02/2008.

rections were always well below the typical level of our polarization detections ($\sim 1-1.5\%$).

Verification of the photometry, calibration and the reduction was done by observation of polarimetric standards. The standard stars observed were NGC 2024-1 and Vela1_95 at VLT (Fossati et al. 2007; Whittet et al. 1992), HD19820 at CAHA (Wolff, Nordsieck & Nook, 1996) HD94851, BD25727, HD251204, and G191B2B at NOT (Turnshek et al. 1990; Schmidt et al. 1992). Table 1 shows the inferred θ and P values, once they were corrected for the GIP and the statistical bias (multiplying P by $\sqrt{1-(\sigma_P/P)^2}$) due to the fact that P is a positive quantity (Wardle & Kronberg 1974).

For some observing epochs we explored maximising the time resolution of our polarimetric monitoring at the expense of enlarging the polarimetric errors. This was done, when possible, by splitting the polarimetric data of one night in cycles of four images, i.e., the minimum block of images necessary to get a polarimetric point. Unfortunately most of the polarization detections showed modest significance levels (between 1.1σ and 4.7 σ), so we could not split the data. Only for the VLT data taken on January 30 the data could be divided in two cycles of four images, whereas still keeping high-significance polarization detections (above 17.5 σ for each of the two cycles). We verified that the joint data acquired on January 30 (composed of two cycles of four images) yields Stokes parametres consistent with the ones obtained when the data of that night are split in two halves. This provided an extra high-quality data-point for the statistical analyses carried out in Sect. 3.2.1 and Sect. 3.2.2.

The V-band polarimetry values synthesized by Maund et al. (2009) for XRF 080109/SN 2008D on January 31.22 and February 15.18 UT, bring us the opportunity to cross-check our results. Our two closest observations, carried out on January 30.2022 and February 11.9326 UT, yield P and θ values fully consistent[5] with Maund et al. (2009). We are aware that this comparative exercise, although satisfactory, is only limited to two epochs close to the lightcurve maximum and exclusively focused on XRF 080109/SN 2008D, since Maund et al. (2009) did not observe SN 2007uy.

2.2. Millimetre observations

XRF 080109/SN 2008D was observed at 1.2 mm on January 25, 28, and 30, 2008 with the MAMBO II bolometer on the IRAM 30m Telescope (see Table 2). The data were reduced following the standard procedure with the *mopsic* data reduction software. In order to estimate the NGC 2770 contribution at 1.2 mm to our previous XRF 080109/SN 2008D observations we measured, on January 31, the flux of two adjacent regions (Adj1 and Adj2). Such regions bracket the XRF 080109/SN 2008D position in the radial direction towards the NGC 2770 nucleus, both at a distance of $\sim 10''$ from XRF 080109/SN 2008D (beam FWHM at 1.2 mm $\sim$ 11″). They were selected sufficiently close to XRF 080109/SN 2008D to have a good estimate of its background emission, but sufficiently far to avoid most of the XRF 080109/SN 2008D flux within the beam. The adjacent 1.2 mm pointings yielded fluxes consistent with those obtained at the XRF 080109/SN 2008D position (see Table 2), implying that the 1.2 mm data are very likely dominated by the NGC 2770 background flux and not by XRF 080109/SN 2008D.

[5] We note that Maund et al. (2009) only report the mean values of θ, i.e., do not report errors for θ. However, the θ mean values they infer are well within our error bars for both epochs.

Table 2. Log of the millimetre observations.

Date[a] 2008, UT	Telescope	Field	Integration time (min)	λ mm	Flux density [mJy/beam]
Jan 25.931	IRAM 30m	SN 2008D	3×20	1.2	2.46 ± 0.54
Jan 28.200	IRAM 30m	SN 2008D	1×20	1.2	2.29 ± 1.20
Jan 30.171	IRAM 30m	SN 2008D	2×20	1.2	1.44 ± 0.60
Jan 25.931-30.171	IRAM 30m	SN 2008D	6×20	1.2	2.03 ± 0.38[b]
Jan 31.925	IRAM 30m	Adj1[c]	2×16	1.2	2.39 ± 0.70
Jan 31.936	IRAM 30m	Adj2[d]	2×16	1.2	2.81 ± 0.71
Jan 23.854	PdB	SN 2008D	1×60	3.3	0.65 ± 0.15
Nov 9.336	PdB	SN 2008D	1×111	2.9	0.03 ± 0.10

a Mean observing epoch.
b Weighted average of the three previous table lines.
c R.A.=$09^h\ 09^m\ 30\overset{s}{.}085$, Dec.=+33° 08′ 29.″98 (J2000).
d R.A.=$09^h\ 09^m\ 31\overset{s}{.}211$, Dec.=+33° 08′ 10.″25 (J2000).

In addition, a 4.3σ detection was achieved on January 23 at 3.3 mm with the Plateau de Bure (PdB) interferometer centered on XRF 080109/SN 2008D (see Table 2) with an observing beam size of $2.''75\times1.''11$. The last millimetre observation was carried out with the PdB on Nov 9.336 UT at 2.9 mm, yielding a 3σ upper limit of 0.30 mJy/beam. This non-detection suggests that the flux detected at 3.3 mm on January 23 mostly originated from XRF 080109/SN 2008D and not from the host galaxy dust.

3. Results

3.1. Properties of the polarizing ISM towards XRF 080109/SN 2008D

The Galactic reddening towards NGC 2770 is very low ($E(B-V)=0.032$; Schlegel et al. 1998), implying a V-band extinction of only $A_V=0.1$ mag (Cardelli et al. 1989). So the contribution of the Galactic dust to the measured 1.2 mm flux is negligible. Thus, assuming that most of the 1.2 mm emission comes from optically thin dust emission in the host galaxy interstellar medium (ISM) towards XRF 080109/SN 2008D, it is possible to roughly estimate the host optical extinction as: $A_V=(1.086\,S_{1.2})/(B_{1.2}(T_{\rm dust})\,\Omega_{mb})\times(\kappa_V/\kappa_{1.2})$. $B_{1.2}(T_{\rm dust})$ is the Planck function of the dust at a temperature $T_{\rm dust}$, Ω_{mb} is the main-beam solid angle, $S_{1.2}$ is the flux density per beam at 1.2 mm, and $\kappa_V/\kappa_{1.2}$ is the ratio of the visual extinction coefficient to the 1.2 mm dust opacity, which was estimated to be $\langle\kappa_V/\kappa_{1.2}\rangle=(4\pm2)\times10^4$ (Kramer et al. 1998).

In order to estimate A_V a value of $T_{\rm dust}$ has to be assumed. Domingue et al. (1999) inferred $T_{\rm dust}=21\pm2$ K for the colder dust component of a set of three spiral galaxies similar to NGC 2770. On the other hand, the spectral energy distribution (SED) of NGC 2770 integrated over the entire galaxy yields $T_{dust}=30\pm5$ K (Thöne et al. 2009). So we adopted both $T_{dust}=21\pm2$ K and $T_{dust}=30\pm5$ K.

Using $S_{1.2}=(2.03\pm0.38)$ mJy/beam (average of the 3 XRF 080109/SN 2008D 1.2 mm pointings in Table 2) and both $T_{\rm dust}=21\pm2$ K and $T_{\rm dust}=30\pm5$ K, we obtain $A_V=0.43\pm0.31$ and $A_V=0.27\pm0.15$, respectively. However, as $S_{1.2}$ corresponds to the flux integrated in the beam along the projected thickness of the host galaxy (which includes contribution from ISM located beyond the XRF), we can only provide an upper limit to A_V. To be conservative, we will assume an extinction of $A_V<0.43+0.31=0.74$, obtained with $T_{\rm dust}=21\pm2$ K. This A_V value is $\sim 0.5-1.8$ mag lower than the line-of-sight

A_V values inferred by other authors based on a broad diversity of techniques (Mazzali et al. 2008; Soderberg et al. 2008; Malesani et al. 2009; Modjaz et al. 2009). An unrealistic temperature of $T_{\rm dust} \sim 10$ K would be necessary to have an A_V value in agreement with the above authors.

This apparent disagreement can be explained by the impossibility to resolve a clumpy host galaxy ISM with our 1.2 mm beam (FWHM=11″). The clumpy ISM would show three main properties; *i*) an ISM composed by cells overimposed on a lower extinction background, *ii*) cells displaying typical angular sizes smaller than the beam size, *iii*) typical angular separation between cells small enough to allow the beam to contain several cells. Given that the extinction determined by the 1.2 mm data is an average of the integrated flux received in the beam, this scenario would explain the higher extinction derived along the XRF line-of-sight (i.e., spectroscopy). On the other hand, condition *iii*) would explain the fact that the pointings around the XRF 080109/SN 2008D position yielded similar 1.2 mm fluxes, and hence extinction values.

We can estimate a rough upper limit of the typical cell sizes as follows. First, we assume that the flux differences (or internal dispersion) between our three 1.2 mm pointings (see Table 2; weighted flux average of XRF 080109/SN 2008D, Adj1 and Adj2) were entirely due to the statistical fluctuations in the average number of cells (N) contained in each beam. In our case the three 1.2 mm pointings yield 2.03 ± 0.38, 2.39 ± 0.70 and 2.81 ± 0.71 mJy/beam, so the dispersion is 0.41 mJy/beam. If the cells are identical and randomly distributed, then the ratio between the average flux and the dispersion of the 3 pointings would be approximately $\sqrt{N}$. In our case the average flux of the 3 pointings (calculated by weighting with the corresponding flux errors) is 2.24 mJy/beam, so this yields $N \sim 30$ cells/beam. However, the dispersion is very likely not only due to statistical fluctuations of N, i.e, the dispersion has probably also an instrumental/calibration/photon-noise component. So the statistical fluctuations due to N would be likely lower than 0.41 mJy/beam and therefore we can only set a lower limit of $N > 30$. On the other hand, in order to match the A_V derived from the 1.2 mm flux with the spectroscopic A_V values reported in the literature, the emitting region (the total area covered by the cells within the beam solid angle) should fill only[6] 10-30% of Ω_{mb}. This would explain the low $A_V < 0.74$ mag derived using the 1.2 mm flux (Kramer et al. 1998) for cells having a line-of-sight spectroscopic extinction of $A_V = 1.2 - 2.5$ mags. Thus, assuming identical circular cells, a NGC 2770 distance of 27 Mpc (Soderberg et al. 2008), and a Ω_{mb} filling factor of 30%, we can impose a maximum cell diameter of $D < 0.16$ kpc. Adopting a beam filling factor of 10%, we would obtain smaller cells, so we consider 0.16 kpc as a robust upper limit. We note that the dominant P is the result of all the material integrated along the line-of-sight, so we can not conclude that P is due to the XRF circumstellar dust.

3.2. Properties of XRF 080109/SN 2008D and SN 2007uy on the Stokes plane

The P and θ values displayed in Table 1 were corrected for the GIP and the polarimetric statistical bias (Wardle & Kronberg 1974). The further polarimetric analysis will deal with the properties of Q and U of both objects on the Stokes plane, so the P bias correction factor (included in Table 1) will not be considered.

[6] For dust temperatures ranging from $T = 21$ to $T = 30$ K.

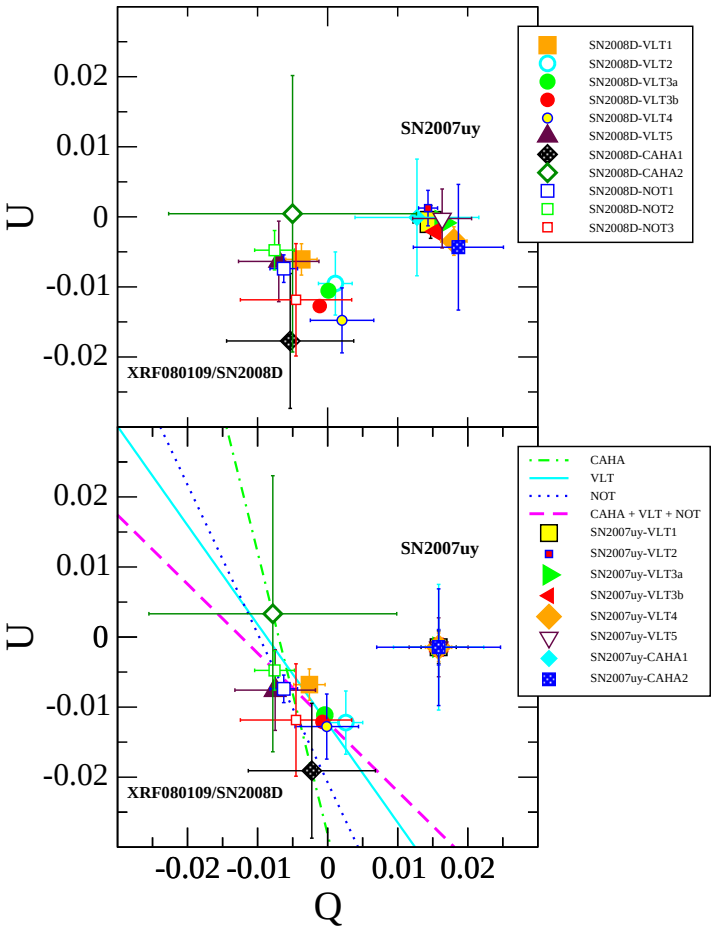

Fig. 1. *Top panel:* Stokes parametres of XRF 080109/SN 2008D and SN 2007uy, once the GIP correction was included. The cloud of measurements representing SN 2007uy seems to be more compact than the XRF 080109/SN 2008D one. *Bottom panel:* Stokes parametres of XRF 080109/SN 2008D and SN 2007uy, if SN 2007uy is kept fixed at its barycentre. The different lines represent the linear fits to the XRF 080109/SN 2008D Stokes parametres obtained when the CAHA (dot-dashed), VLT (continuous), NOT (dotted) and all the data (VLT+CAHA+NOT, long-dashed) are considered. The directions of all the straight lines are statistically consistent (see Table 3), suggesting an instrumental-independent dominant symmetry axis present in the XRF 080109/SN 2008D data.

3.2.1. Is XRF 080109/SN 2008D polarimetrically variable?

The Stokes parametres of XRF 080109/SN 2008D and SN 2007uy, corrected for the GIP, are plotted in Fig. 1. Both events show polarization levels of 1 – 1.5%, significantly lower than the one measured in XRF 060218/SN 2006aj (Gorosabel et al. 2006; Maund et al. 2007). Assuming both a GIP law and a Galactic extinction law (Serkowski et al. 1975; Cardelli et al. 1989) for NGC 2770, the A_V values reported in the literature ($\sim 1.2 - 2.5$ mag) would yield a conservative HGIP polarization upper limit of $P_{max} = 2.9 \times A_V \sim 3.5 - 7.3\%$, consistent with the polarization measured for XRF 080109/SN 2008D and SN 2007uy.

As seen in the top panel of Fig. 1, the cloud of points corresponding to SN 2007uy seems to be more clustered than the one of XRF 080109/SN 2008D. For the two stellar explosions we quantified the probability that the Stokes parametre distri-

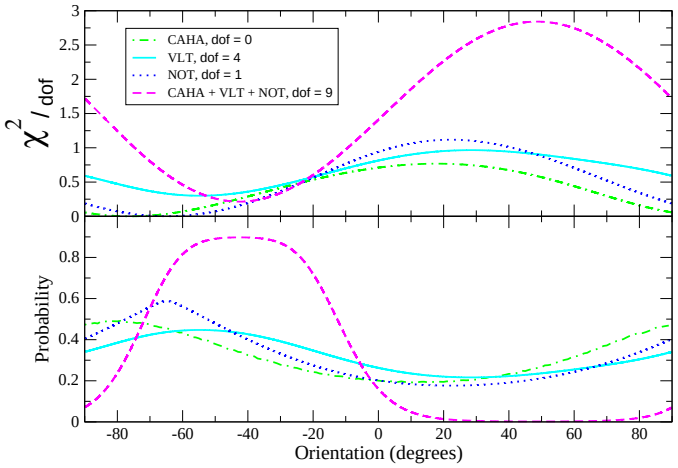

Fig. 2. *Top panel:* The evolution of the linear fit χ^2/dof as a function of the fitted line orientation. The minima correspond to the optimal orientation of the straight lines displayed in the Fig. 1 bottom panel, also given in Table 3. As seen the global shape of the evolution for the three independent data-sets (VLT, NOT and CAHA) are quite equivalent, their minima being systematically located at similar negative angles. The long-dashed line shows the χ^2/dof evolution when all the data are jointly considered. We note that in the case of CAHA, given that dof=0, χ^2/dof represents actually χ^2. *Bottom panel:* The evolution of the normalized probability associated to the above panel. As displayed the three independent data-sets show their probability maxima at a comparable orientation angle. The maximum is reinforced when all the data are combined (long-dashed line). Given that dof=0 for CAHA, the corresponding probability distribution was obtained through a Monte Carlo method. We refer the reader to the main text for further information.

butions are consistent with no time evolution. First, we double checked using Monte Carlo methods that, for the average number of counts of our images, both Q and U follow Gaussian distributions. This fact assures that the χ^2 test is an appropriate statistical tool. Second, we determined the barycentre of the two objects on the Stokes plane ($\langle Q\rangle$, $\langle U\rangle$). Then we calculated for the Q and U of the two events the χ^2/dof value with respect to $\langle Q\rangle$ and $\langle U\rangle$, respectively[7].

For SN 2007uy the distribution of Q (U) shows χ^2/dof=4.19/7 (χ^2/dof=4.32/7) with respect to $\langle Q\rangle$ ($\langle U\rangle$). For XRF 080109/SN 2008D the distribution of Q (U) yields χ^2/dof=19.06/10 (χ^2/dof=22.96/10), clearly larger than the χ^2/dof value of SN 2007uy. These values of χ^2/dof were used to obtain the corresponding probabilities. For SN 2007uy the probability that Q and U are constant are 0.758 and 0.742, respectively. XRF 080109/SN 2008D shows lower probabilities, 0.040 and 0.011, respectively. Thus the probabilities that Q and U are simultaneously constant are 0.563 for SN 2007uy and 4.3×10^{-4} for XRF 080109/SN 2008D.

We are aware that different error sources affecting the measurements (background determination uncertainties, flat field correction inaccuracies, no instrumental polarization correction available along the FoV for the CAHA and NOT images,....) might still not be included in the error bars, so the values of χ^2/dof could be overestimated for both sources (and hence the above probabilities underestimated). Thus, we repeated the exercise augmenting the photometric error bars of both objects and all the field stars by 20%. If we do that, the probability that both Q and U are constant are 0.791 for SN 2007uy and 0.021 for XRF 080109/SN 2008D, respectively.

We have verified if due to some uncontrolled reason the (Q,U) distribution on the Stokes plane is just the result of mixing data acquired with different telescopes/instruments. In order to inspect the existence of this potential instrumental artifact, we redid the statistical analysis separating the images that contain both objects according to the telescope used (hence the NOT is excluded from this comparative study between SN 2007uy and XRF 080109/SN 2008D since SN 2007uy was not imaged by the NOT). Thus we determined separately for the VLT and CAHA the probabilities of having constant Stokes parametres.

Using only the VLT data points, we determined that the probability that both Q and U are constant are 0.295 for SN 2007uy and 0.007 for XRF 080109/SN 2008D, respectively. If we enlarge the photometric errors by 20% the probabilities would be then 0.53 and 0.05, for SN 2007uy and XRF 080109/SN 2008D, respectively. Considering exclusively the CAHA data-set we can not reach strong conclusions given the reduced number of visits (2) and large error bars. However, even with the limited CAHA data, SN 2007uy shows higher probabilities than XRF 080109/SN 2008D of being polarimetrically constant, 0.46 versus 0.40. If the CAHA photometric errors are augmented by 20%, then the probabilities are 0.53 and 0.42 for SN 2007uy and XRF 080109/SN 2008D, respectively.

Independent of the data subset considered and the additional photometric uncertainty introduced, XRF 080109/SN 2008D reiteratively displays lower probabilities than SN 2007uy of being polarimetrically constant. In fact, it is not obvious to explain how non-accounted photometric/calibration/instrumental uncertainties could systematically affect only to the values derived for XRF 080109/SN 2008D and not those of SN 2007uy, which shows consistently a higher degree of clustering on the Stokes plane. All the above arguments seem to suggest that XRF 080109/SN 2008D could show an intrinsic variable polarization component added to the dominant HGIP. This suggestion is reinforced when SN 2007uy is used as a secondary polarimetric standard (see Sect. 3.2.2).

3.2.2. A symmetry axis for XRF 080109/SN 2008D?

Given that both SN 2007uy and XRF 080109/SN 2008D were imaged simultaneously with VLT and CAHA, we can use SN 2007uy as a reference star with constant Stokes parametres. In other words, we can assume, justified by the above probabilities, a constant projected geometry for SN 2007uy plus a constant HGIP. As an additional argument, it is also interesting to note that the agreement between the synthetic broad-band points reported by Maund et al. (2009) and our data is even better when SN 2007uy is fixed on the Stokes plane.

Thus, using SN 2007uy as calibrator, a linear fit to the XRF 080109/SN 2009 data yields a satisfactory χ^2/dof=0.21 (dof=9, long-dashed straight line of Fig. 1 bottom panel). Hence, the XRF 080109/SN 2008D Stokes parametres might suggest the existence of a dominant symmetry axis, offset from the origin due to the HGIP. Furthermore, as seen in the first three lines of Table 3 the inferred symmetry axes show a preference to negative orientations independent of the telescope+instrument employed in the observations[8]. This effect can be seen in the

[7] χ^2_Q/dof = $\sum_{i=0}^{k}(\frac{Q_i-\langle Q\rangle}{\Delta Q_i})^2$ / ($k-1$) and χ^2_U/dof = $\sum_{i=0}^{k}(\frac{U_i-\langle U\rangle}{\Delta U_i})^2$ / ($k-1$), k being the number of visits and dof=$k-1$ the degrees of freedom.

[8] We define the orientation as the angle of the fitted straight line with respect to the horizontal axis representing Q on the Stokes plane. The orientation ranges between -90 and +90 degrees.

Table 3. Linear fits on the Stokes plane of XRF 080109/SN 2008D. The linear fits are shown in the bottom panel of Fig. 1, where we used SN 2007uy as a reference star with constant Stokes parametres. Column 1 displays the telescope used and column 2 the number of visits or points on the Stokes plane. Column 3 provides the χ^2/dof of the optimal linear fit. Column 4 shows the orientation angles at the minima (maxima) of the Fig. 2 upper (bottom) panel. Columns 5 and 6 provide the lower and upper error bars around the orientation angle of the linear fit. As seen the three independent data-sets (CAHA, NOT and VLT) show orientations well consistent within errors. Last table line reports the results when all the data are combined.

Telescope	Number of visits	Minimum χ^2/dof	Orientation angle (degrees)	Lower Error Bar (degrees)	Upper Error Bar (degrees)
CAHA	2	0[a]	-76.1	49.3[b]	48.5[b]
NOT	3	0.001/1	-64.8	46.7	46.0
VLT	6	1.198/4	-54.8	52.1	51.8
CAHA+VLT+NOT	11	1.922/9	-42.6	23.2	22.9

a In this particular case, $\chi^2 = 0$ and dof=0 for the minimum, so χ^2/dof could also be formally represented by 0/0.

b Errors obtained through Monte Carlo methods.

bottom panel of Fig. 1, which shows the linear fits carried out both when the data are considered separately (CAHA, VLT, NOT) and jointly (CAHA+VLT+NOT). The linear fits were obtained minimizing χ^2, which is defined as the weighted distance perpendicular to the fitted line[9]. We considered this χ^2 definition because the variables to be fitted (Q,U) and their corresponding errors are treated symmetrically (Boogs et al. 1990; Babu & Feigelson 1996).

In order to quantify the degree of consistency that the symmetry axes of the 3 data-sets could show, we mapped the evolution of the linear fit χ^2/dof when the orientation of the symmetry axis is varied from −90 to +90 degrees. The upper panel of Fig. 2 shows this evolution. We warn the reader that in the particular case of CAHA dof=0, so what is plotted for CAHA in the Fig. 2 upper panel represents actually χ^2. As seen all the three independent data-sets show their χ^2/dof minima approximately at the same orientation. The position of all the χ^2/dof minima were positively confirmed using the `fitexy` routine implemented by Press et al. (1992). The lower panel of Fig. 2 shows the normalized probabilities corresponding to the χ^2/dof values of the above panel.

For the case of CAHA, given that dof=0, the plotted probability evolution was obtained by simulating mock CAHA Stokes parametres created by a weighted Monte Carlo method assuming Gaussian errors for Q and U. Then given two simulated (Q, U) CAHA pairs the orientation of the line passing through those Stokes parametres is determined. The repetition of this process allowed us to construct the histogram of the line orientations for the CAHA data. Thus, the lower panel of Fig. 2 displays for CAHA the histogram of orientations for 6×10^5 Monte Carlo simulations[10].

For each data-set the upper and lower error bars in the orientation angle (displayed in Table 3, columns 5 and 6) were calculated by integrating the ±34.145% percentile of the probability distribution around the corresponding maximum. As seen in Table 3 the axes inferred from the three independent data-sets are consistent within errors. Hence, the inferred symmetry axes are statistically consistent in all cases, regardless of the instrumental setup used to determine it. It is interesting also to remark that the NOT Stokes parametres, which did not use SN 2007uy as a secondary calibrator (so they might apply a slightly different GIP correction), are also satisfactorily fitted by a straight line. Furthermore, the orientation of the NOT linear fit agrees with the ones inferred based on the VLT and CAHA data. All these arguments strengthens the reality of this possible symmetry axis.

The existence of a symmetry axis on the Stokes plane could be explained by an axisymmetric explosion where the direction of the symmetry axis is constant, but the eccentricity evolves in time. We stress that our polarimetric data can provide exclusively information about the projected geometry on the plane of the sky. Thus, we can not discard that the constant Stokes parametres of SN 2007uy could be caused by a variable eccentricity expansion when it is viewed exactly pole-on.

3.3. Discussion

Maund et al. (2009) report a variation in the position angle of the He I λ5876 line based on comparison of their two observing epochs. Thus, we have to be cautious to explain the origin of the possible XRF 080109/SN 2008D polarization variability. The XRF 080109/SN 2008D polarization variation suggested by the analysis of the broad-band data could not be explained, totally or partially, just by an axisymmetric expansion. We can not discard that the polarization variability could be at some degree caused by the changing relative strengths in the line/continuum emission, only one of which may be polarized, as discussed by Maund et al. (2009). Thus while V-band polarimetric data alone can not resolve these potential components, in principle only spectropolarimetry could study the impact of this, and other possible effects, on the evolution of the Stokes parametres. However, the limited time-coverage of the spectropolarimeric data (only two epochs available, covering 2 weeks around the lightcurve maximum) makes no possible to set strong conclusions about potential effects which could impact our eleven visits spanning $\sim$ 75 days. We can only conclude that our data suggest a preference to an approximately axisymmetric configuration, although we can not exclude deviations from axisymmetry towards a more complex geometry, as discussed by Maund et al. (2009).

Since SN 2007uy occurred earlier than XRF 080109/SN 2008D, we have checked to what degree a possible early fast-evolving epoch of SN 2007uy was missed by our observations. An inspection of the lightcurves of the two events shows that our data cover the rising phase, the maximum and the decay of both objects. The polarization inferred for SN 2007uy in these 3 phases is consistent with

[9] Also known as *weighted total least squares* (WTLS), *weighted rigorous least squares*, or *weighted orthogonal regression* method (see Lemmerling & van Huffel 2002, and references therein).

[10] This Monte Carlo method, used for determining the probability distribution for CAHA, is not optimal for the VLT and NOT data. For the VLT and the NOT a set of simulated Stokes parametres do not determine a line passing through them (they contain more than 2 visits) and a formal fit is necessary. So, the histogram of orientations would mix linear fits with different qualities.

being constant. Obviously, we can not discard that SN 2007uy showed polarization variability earlier than our first epoch, later than the last epoch or in the unavoidable temporal gaps between observations. So, we stress that our conclusions on SN 2007uy and XRF 080109/SN 2008D only refer to the time covered by our observations.

Under the mentioned limitations, the distribution of SN 2007uy on the Stokes plane imposes an upper limit on the intrinsic time-variability of its corresponding Q and U. The weighted Q (U) dispersion of SN 2007uy on the Stokes plane is 1.0×10^{-3} (1.1×10^{-3}). Any possible intrinsic Q (U) variability should be embedded in this dispersion. On the other hand we have determined the maximum intrinsic polarization that our SN 2007uy data could still tolerate. Thus, we have distorted the SN 2007uy Stokes parametres by means of Monte Carlo methods introducing Gaussian shifts in the barycentre of its Stokes parametres. We have determined that with barycentre shifts of $|\Delta Q| \leq 3.8 \times 10^{-4}$ our SN 2007uy data would still be consistent (above 1σ) with no intrinsic polarization in Q. In the same way, for U we have concluded that our SN 2007uy data are insensitive to intrinsic polarization variations with amplitudes below $|\Delta U| \leq 2.2 \times 10^{-4}$. This maximum Q (U) intrinsic variability is approximately one third (fifth) of the Q (U) dispersion of the SN 2007uy Stokes parametres around its barycentre.

4. Conclusions

For both stellar explosions our optical polarization data seem to be dominated by the HGIP. This conclusion is supported by our 1.2 mm observations, performed at and around the XRF 080109/SN 2008D position on NGC 2770. The 1.2 mm measurements are consistent with no intrinsic emission from XRF 080109/SN 2008D at this wavelength, and can be explained by the host galaxy dust emission. The A_V inferred from our 1.2 mm observations is ~ 1.2 mag lower than the line-of-sight extinction values reported in the literature. This apparent contradiction can be solved if the NGC 2770 projected dust distribution around XRF 080109/SN 2008D is composed of dense clumps ($A_V \sim 1.2 - 2.5$ mag) with a typical size < 0.16 kpc and a low filling factor (10-30%) in our 1.2 mm beam.

As a bonus, we also report the detection of 0.65 mJy/beam at 3.3 mm coincident with XRF 080109/SN 2008D 14 days after the X-ray outburst. This emission agrees fairly well with the lightcurve modeled at 95 GHz (Soderberg et al. 2008). Furthermore an observation at 2.9 mm carried out on Nov 9.3 UT 2008 (304.8 days after the XRF), imposed a 3σ flux upper limit of 0.30 mJy/beam, so we conclude that the 3.3 mm detection is mostly intrinsic emission from XRF 080109/SN 2008D.

Notwithstanding the important HGIP, a statistical analysis of the distribution of the XRF 080109/SN 2008D Stokes parametres suggests that XRF 080109/SN 2008D exhibits an intrinsic variable polarization component embedded in the dominant HGIP. In contrast, the SN 2007uy polarization data can be described by a constant projected geometry. This conclusion is achieved independent of the data being considered jointly or separately according to the telescope used.

Assuming that the SN 2007uy projected geometry is constant in time, then the evolution of the XRF 080109/SN 2008D Stokes parametres could show a symmetry axis. This possible symmetry axis is also independent of the instrumentation used to perform the observations, supporting its reality. This potential axis could be approximately explained by an axisymmetric aspherical expansion with variable eccentricity. However, our broadband polarimetric data can not exclude more complex geometric configurations, as possible deviations from axisymmetry. Our results are consistent with the XRF 080109/SN 2008D asphericity inferred from spectroscopic data (Modjaz et al. 2009; Tanaka et al. 2009). We suggest that at least the projected, if not the intrinsic, geometry of the two explosive events could be different.

Acknowledgements. The research of JG, AJCT, MJ and IA is supported by the Spanish programmes ESP2005-07714-C03-03, AYA2004-01515, AYA2007-67627-C03-03, AYA2008-03467/ESP and AYA2009-14000-C03-01. AdUP acknowledges support from an ESO fellowship. AR and SK acknowledge support by DFG Kl 766/11-3, PF and DAK by the Thüringer Landessternwarte. IA acknowledges support by an I3P contract with the Consejo Superior de Investigaciones Científicas (CSIC). We thank M.A. Pérez Torres and L.M. Sarro for fruitful comments. The Dark Cosmology Centre is funded by the DNRF. This paper is based on data from the IRAM 30m telescope, the PdB interferometer, the NOT, the VLT and the 2.2m Telescope of Calar Alto. ALFOSC is owned by Instituto de Astrofísica de Andalucía (IAA) and operated at the NOT under agreement between the IAA and NBIfAFG. We thank the IRAM Director and C. Thum for providing discretionary observing time at the IRAM 30m telescope. The German-Spanish Astronomical Center, Calar Alto, is jointly operated by the MPIA Heidelberg and IAA (CSIC). IRAM is supported by INSU/CNRS (France), MPG (Germany) and IGN (Spain). The VLT data were acquired with target of opportunity programme 080.D-0008(A).

References

Babu, G.J., & Feigelson, E.D., 1996, *"Astrostatistics"*. London: Chapman & Hall
Berger, E., & Soderberg, A.M., 2008, GCN Circ. 7159
Bersier, D., et al., 2003, ApJ, 583, L63
Björnsson, G. et al., 2003, ApJ, 579, L59
Boggs, P.T., Donaldson, J.R., Byrd, R.H., & Schnabel, R.B., 1990, ODRPACK: Software of weighted orthogonal distance regression, *ACM Trans. Math. Software*, 16, 348.
Cardelli, J. A., Clayton, G. C., & Mathis, J. S., 1989, ApJ, 345, 245
Covino, S., et al., 1999, A&A, 351, 399
Covino, S., et al., 2002, A&A, 392, 865
Covino, S., et al., 2003, A&A, 400, L9
Covino, S., 2009, in Proceedings of the conference "The coming of age of X-ray polarimetry", in press, arXiv:0906.5440
di Serego Alighieri, S., 1997, in Instrumentation for Large Telescopes, VII Canary Islands Winter School of Astrophysics, ed. J.M. Rodríguez Espinosa, A. Herrero, & F. Sánchez (Cambridge Univ. Press), 287
Domingue, D. L., et al., 1999, AJ, 118, 1542
Fossati, J., Bagnulo, S., Mason, E., Landi Degl'Innocenti, E. 2007, in The Future of Photometric, Spectrophotometric and Polarimetric Standardization, ed. C. Sterken. ASP Conference Series, Vol. 364, 503
Fynbo, J.P.U., et al., 2009, ApJS, submitted arXiv:0907.3449
Galama, T.J., et al., 1998, Nature, 395, 670
Gorosabel, J., et al., 2004, A&A, 422, 113
Gorosabel, J., et al., 2006, A&A, 459, L33
Greiner, J., et al., 2003, Nature, 426, 157
Hjorth, J., et al., 1999, Science, 283, 2073
Hjorth, J., et al., 2003, Nature, 423, 847
Höflich, P., et al., 1991, A&A, 246, 481
Immler, S. et al., 2008, GCN Circ 7185
Kann, D.A., et al., 2007, ApJ, submitted, arXiv:0712.2186
Kann, D.A., et al., 2008, ApJ, submitted, arXiv:0804.1959
Kasen, D., et al., 2003, ApJ, 593, 788
Kong, A.K.H., & Maccarone, T.J., 2008, The Astronomer's Telegram 1355
Kramer, C., et al., 1998, A&A, 329, L33
Lemmerling, P., & van Huffel, S., 2002, *"Total least squares and errors-in-variables modeling: analysis, algorithms and applications"*, Dordretch, Boston, Kluwer Academic.
MacFadyen, A., & Woosley, S.E., 1999, ApJ, 524, 262
Malesani, D., et al., 2004, ApJ, 609, L5
Malesani, D., et al., 2009, ApJ, 692, L84
Masetti, N,. et al., 2003, A&A, 404, 465
Maund, J. R., et al., 2007, A&A, 475, L1
Maund, J. R., et al., 2009, ApJ, submitted, arXiv:0908.2841
Mazzali, P., et al., 2008, Science, 321, 1185
Modjaz, M., et al., 2009, ApJ, 702, 226
Pian, E., et al., 2006, Nature, 442, 1011
Press, W. H., et al., 1992, Numerical Recipes, 2nd ed, Cambridge Univ. Press
Rol, E., et al., 2003, A&A, 405, L23

Sakamoto, T., et al., 2005, ApJ, 629, 311
Schmidt, G.D., Elston, R., & Lupie, O.L., 1992, AJ, 104, 1563
Schlegel, D.J., Finkbeiner, D.P., & Davis, M., 1998, ApJ, 500, 525
Serkowski, K., Mathewson, D. S. & Ford, V. L., 1975, ApJ, 196, 261
Soderberg, A., et al., 2008, Nature, 453, 469
Sollerman, J., et al., 2006, A&A, 454, 503
Stanek, K. Z., et al., 2003, ApJ, 591, L17
Tanaka, M., et al., 2009, ApJ, 700, 1680
Thöne, C., et al., 2009, ApJ, 698, 1307
Thomsen, B., et al., 2004, A&A, 419, L21
Turnshek, D.A., et al., 1990, AJ 99, 1243
Wang, L., Howell, D. A., Höflich, P., & Wheeler, J. C. 2001, ApJ, 550, 1030
Wang, L. & Wheeler, J. C. 2008, ARA&A, 46, 433
Wardle, J. F. C., & Kronberg, P.P., 1974, ApJ, 194, 249
Whittet, D.C.B. et al., 1992, ApJ, 386, 562
Wolff, M.J., Nordsieck, K.H., Nook, M.A., 1996, AJ 111, 856
Woosley, S. E., 1993, ApJ, 405, 273
Woosley, S. E., & Bloom, J.S., 2006, ARA&A, 44, 507